Available online at www.sciencedirect.com
SCIENCE DIRECT®
Journal of Solid State Chemistry 173 (2003) 342–349
JOURNAL OF SOLID STATE CHEMISTRY
http://elsevier.com/locate/jssc

Crystal structure and cation transport properties of the layered monodiphosphates $Rb_6Bi_4(PO_4)_2(P_2O_7)_3$

C. Falah,[a] H. Boughzala,[a] T. Jouini,[a,*] and A. Madani[b]

[a] *Laboratoire de cristallochimie, Département de chimie, Faculté des Sciences de Tunis, Campus Universitaire, Tunis 1060, Tunisia*
[b] *Département de physique, Faculté des Sciences de Tunis, 7021 Bizerte, Tunisia*

Received 15 October 2002; received in revised form 20 December 2002; accepted 9 February 2003

Abstract

Single crystals of the new Bi(III) phosphates, $Rb_6Bi_4(PO_4)_2(P_2O_7)_3$, have been isolated and their structure has been determined by X-ray diffraction techniques. This compound crystallizes in the monoclinic space group $P2_1/c$ with $a = 9.077(1)$ Å, $b = 9.268(2)$ Å, $c = 36.418(6)$ Å, $\beta = 95.75(1)^\circ$ and $Z = 8$. The crystal structure is made up of BiO_5 and BiO_6 polyhedra sharing the corners with PO_4 tetrahedra and P_2O_7 diphosphate groups. The structure can be described as infinite anionic layers with composition $[Bi_4(PO_4)_2(P_2O_7)_3]^{6-}_{\infty}$ parallel to the [301] plane, connected via P–O–Bi bridges to form a three-dimensional open framework. This framework delimits tunnels running along [100] and [010] directions, where the rubidium ions reside. This compound exhibits a rubidium ion conduction but with rather low conductivity value $\sigma = 2.45 \times 10^{-7}\ \Omega^{-1}\ cm^{-1}$ at 640 K.

Keywords: First monodiphosphate of Bi(III); Open framework; Intersecting tunnels

1. Introduction

It is well established that ions such as Bi^{3+} and Pb^{2+} often generate distorted structures due to the electrostatic effect of the lone pair of electrons. The compounds formed by combination of such ions with tetrahedral anions (VO_4 or PO_4) are promising materials in the field of inorganic material technology and have possible applications as hosts for laser materials [1–3].

Due to these reasons, many works have been devoted to the study of mixed bismuth phosphates. To our knowledge, only few compounds on double phosphate of bismuth and alkali metals have been reported. In the Rb_2O–Bi_2O_3–P_2O_5 system, only $RbBi(PO_3)_4$ phase was characterized by X-ray powder pattern [4].

In the present paper, the preparation and crystal structure data of the new $Rb_6Bi_4(PO_4)_2(P_2O_7)_3$ phase are reported and the crystal structure is described and its Rb^+ ion transport properties were measured.

2. Experimental

The synthesis was carried out in air by a solid-state reaction. A mixture of Rb_2CO_3, Bi_2O_3 and $NH_4H_2PO_4$ with the molar ratio Rb/Bi/P = 5/2/5, intimately mixed, was preheated in an alumina crucible, at 573 K for 12 h in order to eliminate CO_2, NH_3 and H_2O. Then, these ingredients were heated to 873 K for 25 days and cooled to room temperature at the rate of 5°C/h; this led to the formation of the parallelepipedic colourless crystal of $Rb_6Bi_4(PO_4)_2(P_2O_7)_3$.

3. Data collection

A colourless parallelepiped-shaped crystal of approximate dimensions $0.036 \times 0.054 \times 0.072\ mm^3$ was mounted on a Nonius CAD-4 diffractometer to be used for the structure determination. Table 1 lists the main crystal data and refinement parameters for $Rb_6Bi_4(PO_4)_2(P_2O_7)_3$.

A graphite monochromated Mo$K\alpha$ ($\lambda = 0.71069$ Å) beam was used for the data collection. The cell parameters reported in Table 1 were determined and optimised by least-squares refinement based upon 25

*Corresponding author. Fax: +33-56-84-66-34.
E-mail address: tahar.jouini@fst.rnu.tn (T. Jouini).

0022-4596/03/$ - see front matter © 2003 Elsevier Science (USA). All rights reserved.
doi:10.1016/S0022-4596(03)00108-7

Table 1
Crystal data and refinement parameters for $Rb_6Bi_4(PO_4)_2(P_2O_7)_3$

Crystal data	
$Rb_6Bi_4(PO_4)_2(P_2O_7)_3$	Mo$K\alpha$ radiation
$M_r = 1030.3$	$\lambda = 0.71069$ Å
Monoclinic	$\theta = 10-12°$ (for reflexions used to refine cell)
$P2_1/c$	$\mu = 33.07\,mm^{-1}$
$a = 9.077(1)$Å	$T = 298(2)$ K
$b = 9.268(2)$ Å	Parallelepiped
$c = 36.418(6)$ Å	$0.036 \times 0.054 \times 0.072\,mm^3$
$\beta = 95.75(1)°$	Colourless
$V = 3048.2(2)$ Å^3	$D_x = 4.49$
$Z = 8$	
Intensity measurement	
Diffractometer CAD-4	$R_{int} = 0.0434$
Scan mode $\omega/2\theta$	$\theta_{max} = 22°$
Absorption correction by ψ-scan	$h = -7 \rightarrow 7$
$T_{min} = 0.2129$; $T_{max} = 0.2213$	$k = 0 \rightarrow 8$
2133 measured reflections	$l = 0 \rightarrow 31$
2085 independent reflections	1408 reflections $I > 2\sigma(I)$
Refinement	
$R = 0.0521$	$\Delta\rho_{max} = 2.028e$ Å^{-3}
w$R = 0.1067$	$\Delta\rho_{min} = -1.520e$ Å^{-3}
Goof = 1.095	Extinction correction: SHELXL97
2085 reflections	Extinction coefficient: 0.00011(3)
240 parameters	Atomic scattering factors from International Tables for Crystallography (Vol. C)
$w = 1/[\sigma^2(F_0^2) + (0.044P)^2 + 56.1780P]$	
$P = (F_0^2 + 2F_c^2)/3$	

reflections $10° < \theta < 12°$. Raw data were corrected for Lorentz, polarization effects and an empirical absorption correction using ψ-scan [5] method was applied. Scattering factors for neutral atoms were taken from the "International Tables for X-ray Crystallography".

4. Structure determination

The systematic absence conditions in the reduced data ($h\,0\,l$, $l = 2n$, $0\,k\,0$, $k = 2n$) were consistent with the space group $P2_1/c$ (No. 14). The refinements were based on F^2; the heavy-atom method carried out using SHELXS [6] gave the bismuth and rubidium positions; the subsequent Fourier synthesis allowed to locate phosphorus and oxygen atoms. The final cycle of refinement [7] of all positional parameters, anisotropic thermal parameters of Rb and Bi atoms and isotropic extinction coefficients led to $R = 0.0521$ and $R_w = 0.1067$, respectively. At this stage, final Fourier difference maps revealed no additional atomic sites.

Table 2
Atomic coordinates and U_{eq} for $Rb_6Bi_4(PO_4)_2(P_2O_7)_3$

Atoms	x/a	y/b	z/c	U_{eq}
Bi1	0.3644(2)	0.0873(2)	0.05478(4)	0.0144(6)
Bi2	0.0580(2)	0.2929(2)	0.12246(5)	0.0137(6)
Bi3	0.1792(2)	0.6162(2)	0.05206(4)	0.0119(6)
Bi4	0.4340(2)	0.1247(2)	0.18901(5)	0.0271(6)
Rb1	0.5806(5)	−0.2123(5)	0.1242(1)	0.0306(1)
Rb2	0.3134(5)	0.5033(5)	−0.0495(1)	0.026(1)
Rb3	0.1367(4)	0.0277(4)	−0.0485(1)	0.021(1)
Rb4	0.2822(7)	0.6194(6)	0.1974(2)	0.089(2)
Rb5	−0.0919(5)	−0.0504(5)	0.1904(1)	0.040(2)
Rb6	0.7692(5)	−0.5250(5)	0.2024(1)	0.040(2)
P1	0.459(1)	−0.201(1)	0.0167(3)	0.011(3)
P2	0.060(1)	0.296(1)	0.0234(3)	0.010(3)
P3	0.414(1)	0.387(2)	0.1188(3)	0.028(4)
P4	0.687(2)	0.208(1)	0.1288(4)	0.036(4)
P5	−0.022(1)	0.664(1)	0.124(3)	0.009(3)
P6	0.191(1)	−0.04(1)	0.1204(3)	0.022(3)
P7	0.121(1)	0.234(2)	0.2237(3)	0.032(4)
P8	0.399(1)	0.340(2)	0.2620(5)	0.050(5)
O1	0.573(3)	−0.169(3)	0.0474(7)	0.032(8)
O2	0.374(2)	−0.347(3)	0.0230(7)	0.014(7)
O3	0.521(3)	−0.230(3)	−0.0218(7)	0.028(8)
O4	0.347(2)	−0.072(3)	0.0116(6)	0.008(7)
O5	0.156(3)	0.421(3)	0.0120(7)	0.019(7)
O6	0.155(2)	0.158(2)	0.0284(6)	0.008(7)
O7	−0.008(2)	0.323(2)	0.0596(6)	0.009(7)
O8	−0.060(2)	0.263(2)	−0.0075(6)	0.005(6)
O9	0.431(7)	0.536(7)	0.114(2)	0.17(2)
O10	0.310(3)	0.324(3)	0.0890(8)	0.044(9)
O11	0.365(4)	0.337(4)	0.155(1)	0.06(1)
O12	0.563(5)	0.282(5)	0.110(1)	0.11(2)
O13	0.66(1)	0.07(1)	0.108(3)	0.31(5)
O14	0.820(4)	0.302(3)	0.1233(9)	0.05(1)
O15	0.671(3)	0.192(3)	0.1703(8)	0.043(9)
O16	−0.140(3)	0.674(3)	0.1485(8)	0.041(9)
O17	−0.063(3)	0.687(3)	0.0837(7)	0.018(7)
O18	0.073(3)	0.530(3)	0.1307(7)	0.027(8)
O19	0.104(3)	−0.216(3)	0.1384(8)	0.035(9)
O20	0.324(3)	−0.068(3)	0.1474(8)	0.05(1)
O21	0.235(3)	−0.148(4)	0.0845(9)	0.06(1)
O22	0.085(3)	0.035(3)	0.1140(8)	0.044(9)
O23	0.014(4)	0.201(3)	0.251(1)	0.06(1)
O24	0.046(3)	0.297(3)	0.1882(9)	0.05(1)
O25	0.220(3)	0.101(3)	0.2157(7)	0.029(8)
O26	0.231(3)	0.351(3)	0.2423(8)	0.045(9)
O27	0.403(4)	0.260(4)	0.294(1)	0.06(1)
O28	0.488(4)	0.293(3)	0.2329(9)	0.05(1)
O29	0.439(5)	0.503(5)	0.265(1)	0.10(2)

Table 2 reports atom positions and equivalent thermal factors. Selected distances and angles are listed in Table 3.

5. Results and discussion

The crystal structure is made up of BiO_5 and BiO_6 polyhedra sharing corners with PO_4 tetrahedra and P_2O_7 diphosphate groups. The structure can be

Table 3
Interatomic distances (Å) at angles (°) in $Rb_6Bi_4(PO_4)_2(P_2O_7)_3$

Tetrahedron $P1O_4$		Tetrahedron $P2O_4$		Polyhedron $Bi1O_5$	
P1–O1	1.47(3)	P2–O8	1.52(3)	Bi1–O3^a	2.12(3)
P1–O4	1.59(2)	P2–O5	1.52(2)	Bi1–O6	2.15(2)
P1–O3	1.59(3)	P2–O7	1.53(2)	Bi1–O4	2.15(2)
P1–O2	1.59(2)	P2–O6	1.54(2)	Bi1–O10	2.59(3)
⟨P1–O⟩ = 1.55(3)		⟨P2–O⟩ = 1.53(3)		Bi1–O21	2.74(3)
				⟨Bi1–O⟩ = 2.35(3)	
O1–P1–O4	112(2)	O8–P2–O5	111(1)		
O1–P1–O3	116(2)	O8–P2–O7	110(1)	O3^a–Bi1–O6	91.0(9)
O1–P1–O2	109(1)	O8–P2–O6	112(1)	O3^a–Bi1–O4	90.7(9)
O4–P1–O3	102(1)	O5–P2–O7	106(1)	O3^a–Bi1–O10	82(1)
O4–P1–O2	110(1)	O5–P2–O6	110(1)	O3^a–Bi1–O21	166(1)
O3–P1–O2	108(1)	O7–P2–O6	108(1)	O6–Bi1–O4	83.1(8)
				O6–Bi1–O10	157.4(9)
Tetrahedron $P3O_4$		Tetrahedron $P4O_4$		O6–Bi1–O21	75.6(9)
P3–09	1.40(6)	P4–O12	1.45(5)	O4–Bi1–O10	75.7(8)
P3–010	1.48(3)	P4–O13	1.45(5)	O4–Bi1–O21	91.5(9)
P3–011	1.53(4)	P4–O14	1.51(3)	O10–Bi1–O21	112.1(9)
P3–012	1.71(5)	P4–O15	1.53(3)		
⟨P3–O⟩ = 1.53(5)		⟨P4–O⟩ = 1.48(5)		Polyhedron $Bi2O_6$	
				Bi2–O14^h	2.17(3)
O9–P3–O10	112(3)	O12–P4–O13	96(4)	Bi2–O18	2.21(3)
O9–P3–O11	116(3)	O12–P4–O14	120(2)	Bi2–O7	2.32(2)
O9–P3–O12	115(3)	O12–P4–O15	113(5)	Bi2–O24	2.39(3)
O10–P3–O11	109(2)	O13–P4–O14	104(4)	Bi2–O22	2.43(3)
O10–P3–O12	96(2)	O13–P4–O15	111(4)	Bi2–O10	2.73(3)
O11–P3–O12	107(2)	O14–P4–O15	110(2)	⟨Bi2–O⟩2.38(3)	
P3–O12–P4 = 141.93(1)					
				O14^h–Bi2–O18	90(1)
Tetrahedron $P5O_4$		Tetrahedron $P6O_4$		O14^h-Bi2-O7	82(1)
P5–O17	1.47(3)	P6–O21	1.50(3)	O14^h–Bi2–O24	81(1)
P5–O16	1.48(3)	P6–O20	1.50(3)	O14^h–Bi2–O22	99(1)
P5–O18	1.53(3)	P6–O22	1.53(3)	O14^h–Bi2–O10	153(1)
P5–O19^j	1.64(3)	P6–O19	1.56(3)	O18–Bi2–O7	91.2(9)
⟨P5–O⟩ = 1.53(3)		⟨P6–O⟩ = 1.53(3)		O18–Bi2–O24	81(1)
				O18–Bi2–O22	171(1)
O17–P5–O16	117(2)	O21–P6–O20	110(2)	O18–Bi2–O10	85(1)
O17–P5–O18	112(2)	O21–P6–O22	110(2)	O7–Bi2–O24	160.7(9)
O17–P5–O19^j	106(2)	O21–P6–O19	109(2)	O7–Bi2–O22	91.1(9)
O16–P5–O18	112(2)	O20–P6–O22	115(2)	O7–Bi2–O10	71.7(8)
O16–P5–O19^j	109(2)	O20–P6–O19	105(2)	O24–Bi2–O22	99(1)
O18–P5–O19^j	98(1)	O22–P6–O19	106(2)	O24–Bi2–O10	124.8(9)
P5–O19–P6 = 135.28(1)				O22–Bi2–O10	87.2(9)
Tetrahedron $P7O_4$		Tetrahedron $P8O_4$		Polyhedron $Bi3O_5$	
P7–O23	1.51(4)	P8–O27	1.39(4)	Bi3–O8^e	2.17(2)
P7–O24	1.53(3)	P8–O28	1.45(3)	Bi3–O2^j	2.18(2)
P7–O25	1.57(3)	P8–O29	1.55(4)	Bi3–O5	2.32(3)
P7–O26	1.58(3)	P8–O26	1.62(3)	Bi3–O21^j	2.52(3)
⟨P7–O⟩ = 1.54(3)		⟨P8–O⟩ = 1.51(4)		Bi3–O17	2.66(2)
				⟨Bi3–O⟩ = 2.37(2)	
O23–P7–O24	113(2)	O27–P8–O28	120(2)		
O23–P7–O25	107(2)	O27–P8–O29	116(3)	O8^e–Bi3–O2^j	85.6(9)
O23–P7–O26	111(2)	O27–P8–O26	111(2)	O8^e–Bi3–O5	85.8(8)
O24–P7–O25	108(2)	O28–P8–O29	103(2)	O8^e–Bi3–O21^j	87.9(9)
O24–P7–O26	111(2)	O28–P8–O26	105(2)	O8^e–Bi3–O17	79.9(8)
O25–P7–O26	107(2)	O29–P8–O26	100(2)	O2^j–Bi3–O5	80.9(9)
				O2^j–Bi3–O21^j	88(1)
				O2^j–Bi3–O17	156.5(9)
Polyhedron $Rb1O_7$		Polyhedron $Rb2O_{10}$		O5–Bi3–O21^j	167(1)
Rb1–O9^f	2.70(6)	Rb2–O5	2.90(3)	O5–Bi3–O17	116(8)
Rb1–O16^b	2.81(3)	Rb2–O2^j	2.98(2)	O21^j–Bi3–O17	73.6(9)
Rb1–O1	2.81(3)	Rb2–O17^e	3.05(2)		
Rb1–O13	2.84(1)	Rb2–O7^e	3.19(2)	Polyhedron $Bi4O_6$	

Table 3 (*continued*)

Tetrahedron $P1O_4$		Tetrahedron $P2O_4$		Polyhedron $Bi1O_5$	
Rb1–O20	2.88(3)	Rb2–O3^{j}	3.21(3)	Bi4–O28	2.25(3)
Rb1–O27^{n}	2.97(4)	Rb2–O2^{a}	3.24(2)	Bi4–O29^{n}	2.25(4)
Rb1-O21	3.37(3)	Rb2-O12^{k}	3.24(5)	Bi4–O25	2.27(3)
$\langle$Rb1–O$\rangle$ = 2.91(3)		Rb2–O1^{a}	3.26(3)	Bi4–O11	2.37(3)
		Rb2–O14^{k}	3.36(3)	Bi4–O15	2.40(3)
Polyhedron $Rb3O_{10}$		Rb2–O9^{k}	3.49(6)	Bi4–O20	2.48(3)
Rb3–O4	2.89(2)	$\langle$Rb2–O$\rangle$ = 3.19(3)		$\langle$Bi4–O$\rangle$ = 2.34(3)	
Rb3–O1^{a}	2.96(3)				
Rb3–O17^{e}	2.97(3)	Polyhedron $Rb4O_{10}$		O28–Bi4–O29^{n}	76(1)
Rb3–O22^{d}	3.02(3)	Rb4–O29	2.94(4)	O28–Bi4–O25	84(1)
Rb3–O6	3.03(2)	Rb4–O19^{j}	2.98(3)	O28–Bi4–O11	80(1)
Rb3–O13^{a}	3.1(1)	Rb4–O26	3.02(3)	O28–Bi4–O15	84(1)
Rb3–O8	3.27(2)	Rb4–O18	3.03(3)	O28–Bi4–O20	167(1)
Rb3–O6^{d}	3.30(2)	Rb4–O27*g*	3.14(3)	O29^{n}–Bi4–O25	91(1)
Rb3–O7^{d}	3.47(2)	Rb4–O11	3.14(3)	O29^{n}–Bi4–O11	153(1)
Rb3–O8^{d}	3.49(2)	Rb4–O20^{j}	3.47(3)	O29^{n}–Bi4–O15	86(1)
$\langle$Rb3–O$\rangle$ = 3.15(2)		Rb4–O23^{o}	3.50(4)	O29^{n}–Bi4–O20	104(1)
		Rb4–O28^{g}	3.51(3)	O25–Bi4–O11	96(1)
Polyhedron $Rb5O_{10}$		Rb4–O9	3.52(6)	O25–Bi4–O15	168(1)
Rb5–O16^{f}	2.99(3)	$\langle$Rb4–O$\rangle$ = 3.23(4)		O25–Bi4–O20	83(1)
Rb5–O26^{m}	3.03(3)			O11–Bi4–O15	81(1)
Rb5–O19	3.11(3)	Polyhedron $Rb6O_8$		O11–Bi4–O20	102(1)
Rb5–O15^{h}	3.15(3)	Rb6–O16^{b}	2.88(3)	O15–Bi4–O20	109(1)
Rb5–O23^{m}	3.18(3)	Rb6–O15^{f}	2.98(3)		
Rb5–O25	3.21(3)	Rb6–O27^{n}	3.09(4)		
Rb5–O23	3.28(3)	Rb6–O24^{b}	3.10(3)		
Rb5–O27^{m}	3.41(3)	Rb6–O25^{n}	3.19(3)		
Rb5–O22	3.43(3)	Rb6–O23^{n}	3.22(3)		
Rb5–O24	3.47(3)	Rb6–O28^{f}	3.34(3)		
$\langle$Rb5–O$\rangle$ = 3.25(3)		Rb6–O14^{f}	3.36(3)		
		$\langle$Rb6–O$\rangle$ = 3.15(3)			

a : $-x+1,-y,-z$; *e* : $-x,-y+1,-z$; *i* : $x-1,y+1,z$; *m* : $-x,y-\frac{1}{1},-z+\frac{1}{2}$; *b* : $x+1$,*y*−1,*z*; *f* : *x*,*y*−1,*z*; *j* : *x*,*y*+1,*z*; *n* : $-x+1,y-\frac{1}{2},-z+\frac{1}{2}$; *c* : $x+1$,*y*,*z*; *g* : $-x+1,y+\frac{1}{2},-z+\frac{1}{2}$; *k* : $-x+1,-y+1,-z$; *o* : $-x,y+\frac{1}{2},-z+\frac{1}{2}$; *d* : $-x,-y,-z$; *h* : $x-1$,*y*,*z*; *l* : $-x+1,y-3/1,-z+\frac{1}{2}$; *p* : $-x+1$, $y+\frac{3}{2},-z+\frac{1}{2}$.

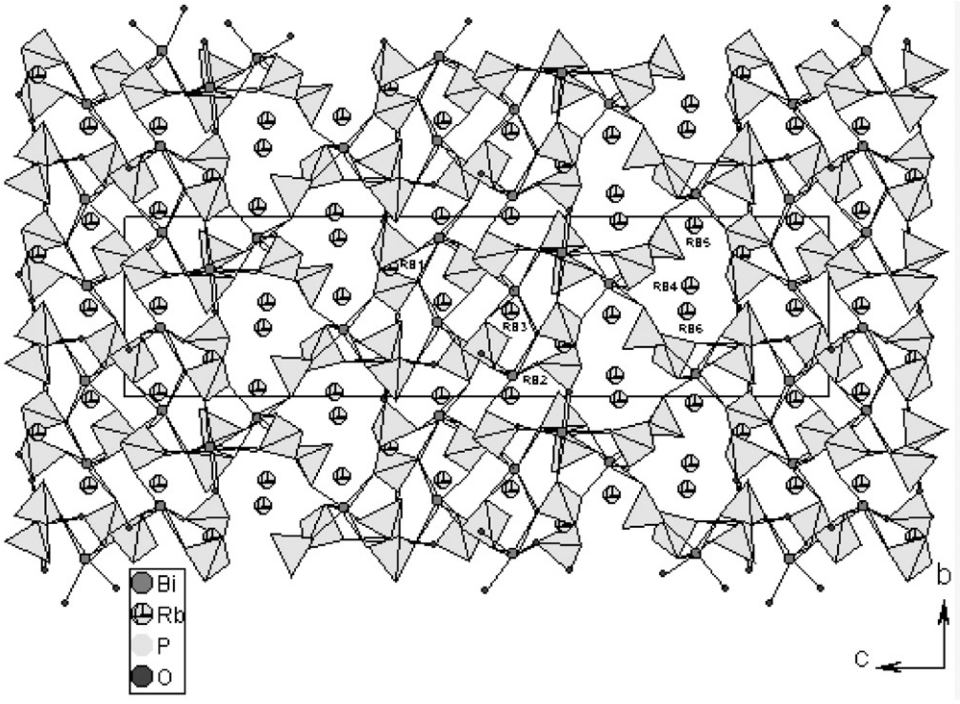

Fig. 1. Projection of the framework of $Rb_6Bi_4(PO_4)_2(P_2O_7)_3$ parallel to [100].

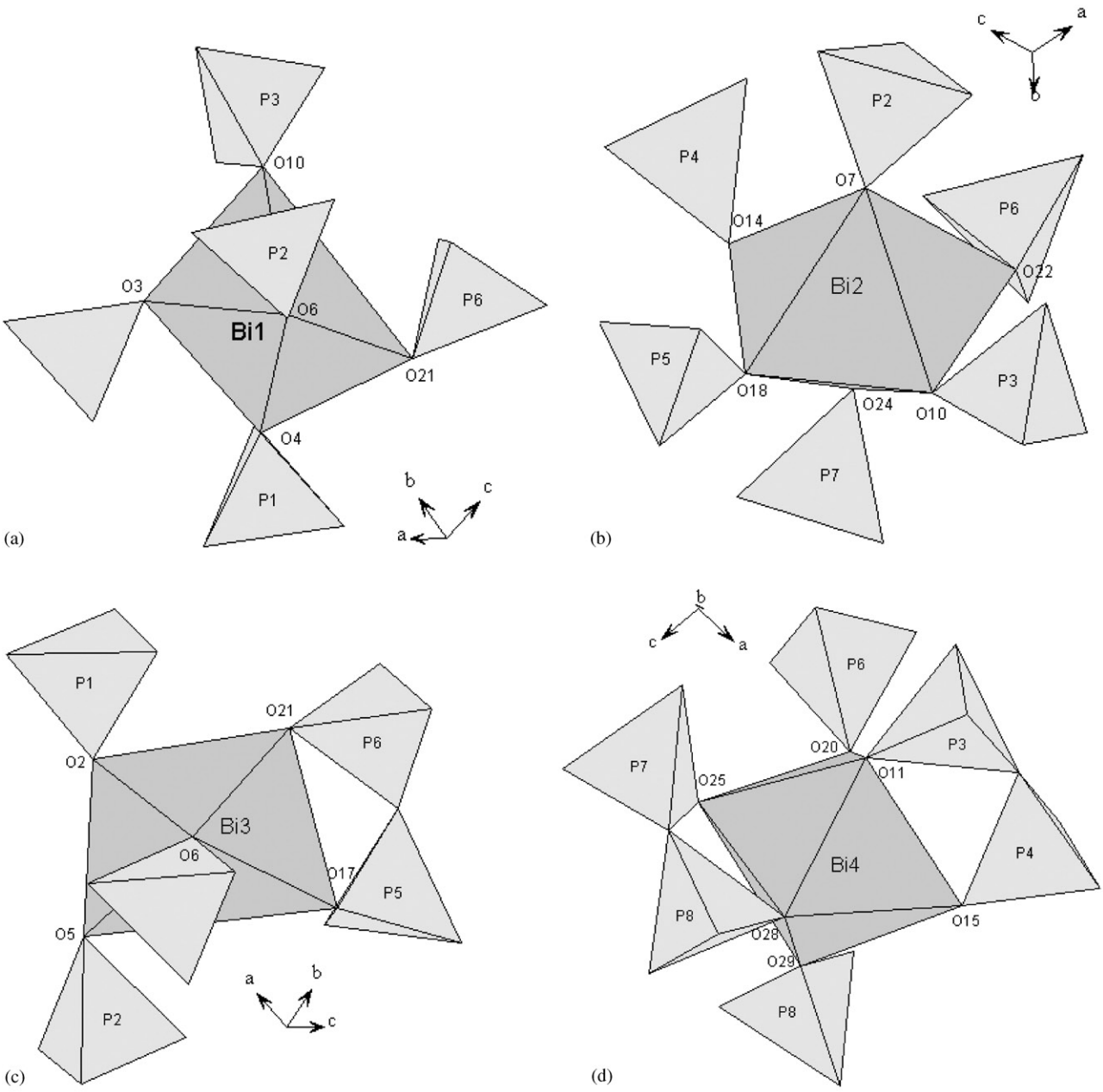

Fig. 2. Bi^{3+} environments.

described as infinite anionic layers with composition $[Bi_4(PO_4)_2(P_2O_7)_3]^{6-}_{\infty}$ parallel to (301) plane, connected via P–O–Bi bridges, to form a three-dimensional framework. This framework delimits tunnels running along [100] and [010] directions where the rubidium ions reside (Fig. 1).

Taking into account the Bi–O bonds shorter than 3 Å, Bi(2) and Bi(4) oxygen polyhedra consist of six atoms forming strongly distorted octahedra (Fig. 2), whereas the coordination number for Bi(1) and Bi(3) is five. The usual low-symmetry environment for Bi^{3+} cations is in fact to be completed by the $6s^2$ stereoactive lone-pair E. This effect is especially pointed out around Bi(1) and Bi(3) which are coordinated by three shortly bonded oxygen atoms at the one side, 2.12(3) Å < Bi–O < 2.32(3) Å, whereas O(10), O(17) and O(21) are longly bonded at the other side which would host E. The Bi(2) and Bi(4) atoms in the asymmetric unit exhibit distorted octahedral coordination, with two shorter Bi–O distances (2.17(3)–2.25(4)Å), two intermediate distances (2.27(3)–2.39(3)Å), three relatively longer Bi–O distances and one longer distance (Bi(2)–O = 2.73(3) Å), characteristic of the triply bonded oxygen, between P_2O_7 group, $Bi(1)O_5$ and $Bi(2)O_6$ polyhedra.

The neighbourhood of $Bi(4)O_6$ octahedra consists of four P_2O_7 units. Two of the P_2O_7 groups are bonded to

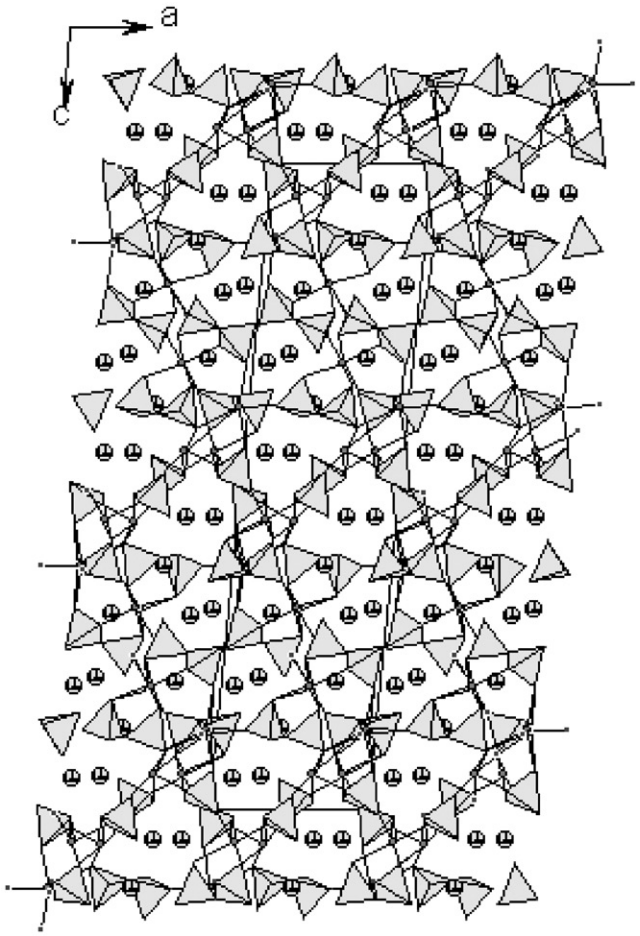

Fig. 3. Projection of the framework of $Rb_6Bi_4(PO_4)_2(P_2O_7)_3$ parallel to [010].

Bi(4) through bidentate bonding and the other two are monodentate. Each $Bi(2)O_6$ octahedron is linked to one single $P(2)O_4$ and five different P_2O_7 units. The $Bi(1)O_5$ pyramidal links corners with three monophosphate tetrahedral and two diphosphate groups, whereas the $Bi(3)O_5$ pyramidal polyhedron shares two oxygen atoms O(17) and O(21) with $P(5)P(6)O_7$ diphosphate group and is also linked to three-monophosphates tetrahedral. In other words, Bi is chelated by a P_2O_7 group as observed in many compounds such as $NaFeP_2O_7$ II [8], $KAlP_2O_7$ [9] and $Na_5Bi(P_2O_7)_2$ [10]. The bond valence sum of Bi–O using Brown formula [11] are 3.07, 3.26, 2.74 and 3.23 for Bi(1), Bi(2), Bi(3) and Bi(4), respectively.

The $P(1)O_4$ monophosphate group show a distorted tetrahedral environment with one shorter distance (P(1)–O(1) = 1.47(3) Å) and three longer distances (1.57(3)–1.59(3) Å).

The $P(2)O_4$ monophosphate tetrahedron exhibits an almost regular tetrahedral geometry and is characterized by four very close P(2)–O distances ranging from 1.52(3) to 1.54(2) Å.

Like in many diphosphates [12], the longest P–O distance in the $P(5)P(6)O_7$ and $P(7)P(8)O_7$ groups corresponds to the bridging oxygen O(19) and O(26), respectively, while the shortest one involves the terminal oxygen atoms, but the average values are comparable to the 1.536 Å value given by Corbridge [13].

The $P(3)P(4)O_7$ diphosphate exhibits one longer bond P(3)–O(12) of 1.71(5) Å and one shorter distance P(4)–O(12) of 1.45(5) Å, of the P–O–P bridging bonds, and the P(3)–O(12)–P(4) angle is 141.93(1)°. These values are

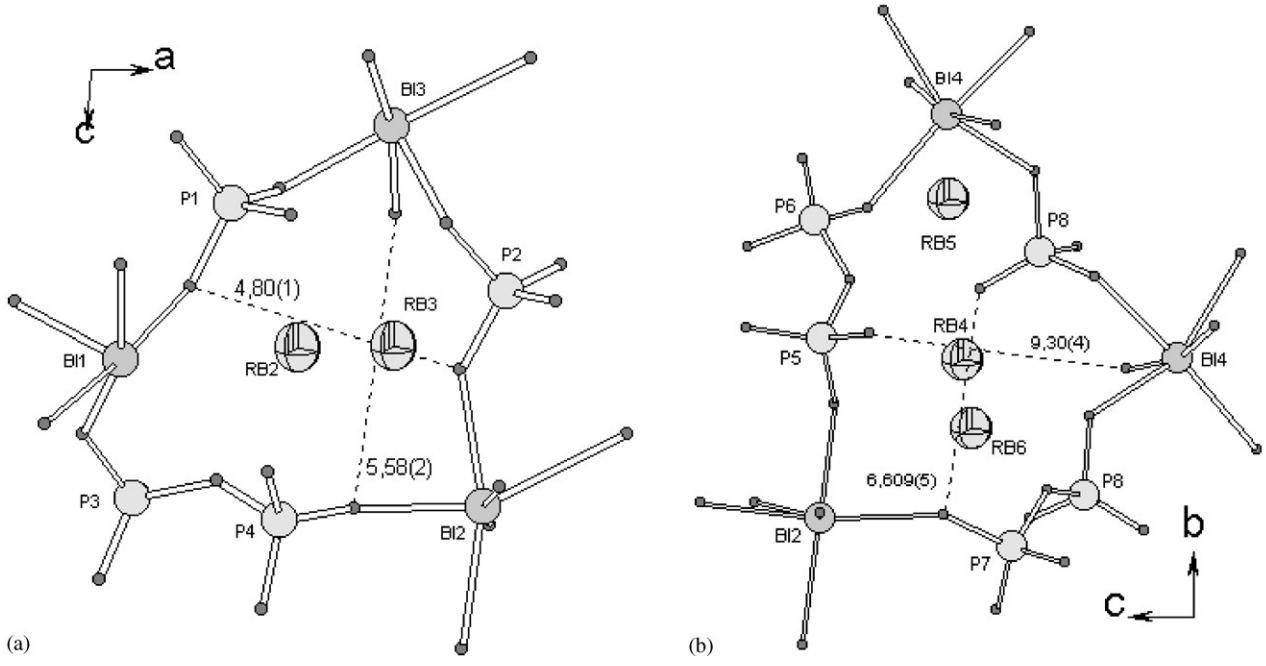

Fig. 4. View of the shape and size of the [010] and [100] tunnel sections.

out of the usual range; this is probably a consequence of acting as bidentate ligand in this structure. A similar situation was found in $Fe_4(P_2O_7)_3$ [14], which shows 1.36(3) and 1.70(1) Å distances values.

Besides, the three-dimensional open anionic framework of this structure contains large intersecting channels, extending along the [100] and [010] directions, wherein the rubidium cations are located (Fig. 3). There are six crystallographically independent rubidium atoms in the structure. Four of them are ten-coordinated and two (Rb(1) and Rb(6)) are surrounded by seven and eight oxygen atoms, respectively. The bond valence sums of Rb–O bonds, ranging from 2.70(6) to 3.52(6) Å, using Brown and Altermatt's data [11], are 1.36, 0.88, 1.04, 0.88, 0.81 and 0.81, for Rb(1), Rb(2), Rb(3), Rb(4), Rb(5) and Rb(6), respectively. Thus the high valence bond sums of Bi(2) and Bi(4) (3.26 and 3.23 respectively) appear to compensate for the decrease of those of Rb atoms. The bond strength sums for the Rb(4), Rb(5) and Rb(6) are lower than the expected value +1, suggesting that the tunnels appear too big for these ions. Sections of the tunnels are shown in Fig. 4.

The title compound of $Rb_6Bi_4(PO_4)_2(P_2O_7)_3$ is the first Bi(III) phosphate built up from monophosphate and diphosphate groups. To our knowledge, among the compounds in the system A–M^{III}–X–O (A = a monovalent or divalent cation; M^{III} = Fe, V, Cr, In, Bi, etc.; X = P, As), only a few contain both monophosphate and diphosphate or monoarsenate and diarsenate groups: $AgV_2(PO_4)(P_2O_7)$ [15], $Ca_2V(PO_4)(P_2O_7)$ [16], $Ba_2Fe_3H(PO_4)_2(P_2O_7)_2$ [17], $Ba_2V_3H(PO_4)_2(P_2O_7)_2$ [17], $Na_7Fe_4(PO_4)(P_2O_7)_4$ [18] and $Na_5Bi_2(AsO_4)(As_2O_7)$ [19].

Table 4
Conductivity result measurement values

Temperature (K)	Z_0 (Ω)	σ (Ω^{-1} cm^{-1})	$1000/T$	$\ln(\sigma T)$
617	904309	1.08×10^{-7}	1.621	−9.629
630	570179	1.71×10^{-7}	1.587	−9.182
640	398549	2.45×10^{-7}	1.563	−8.836
655	521928	1.87×10^{-7}	1.527	−8.560
660	215273	4.54×10^{-7}	1.515	−8.317

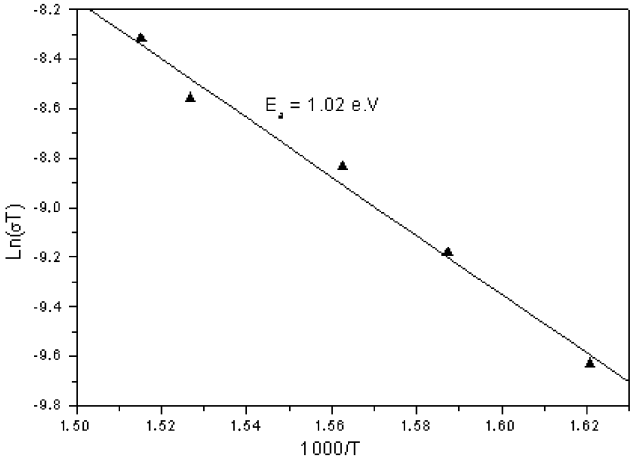

Fig. 5. Arrhenius plot of conductivity for $Rb_6Bi_4(PO_4)_2(P_2O_7)_3$.

6. Cation transport properties

The structural features of $Rb_6Bi_4(PO_4)_2(P_2O_7)_3$ open framework and the location of the rubidium ions in the tunnels, suggest the potential ability of this material to exhibit fast alkali-ion mobility and/or ion-exchange properties.

The sample is obtained by pressing the crystal powder at 12 ton and heating at 773 K for 24 h. It is placed between two blocking electrodes in a tubular furnace, submitted to a temperature regulator.

Conductivity measurements were carried out in the temperature range 617–660 K with 5–15° steps on $Rb_6Bi_4(PO_4)_2(P_2O_7)_3$ by the complex impedance method using a computer-driven Hewlett-Packard 4192A impedance analyser.

Conductivity results measurement lead to the values listed in Table 4. Arrhenius plot of conductivity for $Rb_6Bi_4(PO_4)_2(P_2O_7)_3$ is presented in Fig. 5.

Table 5
Conductivity σ (Ω^{-1} cm^{-1}) and conduction activation energy E_a (eV) of other compounds

Compounds	Température range (K)	σ (Ω^{-1} cm^{-1})	E_a (eV)	Ref.
$Rb_6Bi_4(PO_4)_2(P_2O_7)_3$	617–660	4.54×10^{-7}	1.02	[a]
$Na_3Bi_2(PO_4)_3$	500–750	8.21×10^{-5}	0.882	20
$Li_3NaMo_3O_3(PO_4)_3(P_2O_7)$	573	4.1×10^{-5}	0.89	21
$Li_{3,2}Cs_{0,8}Mo_3O_3(PO_4)_3(P_2O_7)$	573	1.3×10^{-5}	0.79	21
$Li_3Fe_2(PO_4)_3$	400–600	10^{-2}	0.44	22
$Na_3Sc_2(PO_4)_3$	400–600	5.1×10^{-2}	0.34	22
K^+ β-alumine	573	6.5×10^{-4}	0.29	23
$Na_3Zr_2PSi_2O_{12}$	573	2.0×10^{-1}	0.29	24

[a] Present paper.

This material show low conductivity performances, as compared to other compounds [20–24] in Table 5; this probably can be explained by other unfavourable structure features: Rb(1) and Rb(3) lie in too small tunnels as mentioned in the discussion above and all the other rubidium ions are lying with completely occupation site.

7. Concluding remarks

The title compound $Rb_6Bi_4(PO_4)_2(P_2O_7)_3$ is the first Bi(III) phosphate built up from monophosphate and diphosphate groups. The three-dimensional open anionic framework of this structure contains large intersecting channels, extending along the [100] and [010] directions, wherein the rubidium cations are located. These interesting structural features suggest the potential ability of this material to exhibit fast alkali-ion mobility and/or ion-exchange properties. However, this material shows low conductivity performances, this probably can be explained by other unfavourable structure features such as full site occupation by the rubidium atoms and the small dimensions of the tunnels.

References

[1] H.Y.-P. Hong, S.R. Chinn, Mater. Res. Bull. 11 (1976) 421.
[2] V.H. Wulff, B. Finke, L. Schwarz, Z. Phys. Chem. 262 (1981) 1155.
[3] M. Vlasse, C. Parent, R. Salmon, G. Le Flem, P. Hagenmuller, J. Solid State Chem. 35 (1980) 318.
[4] R. Faustova, Inorg. Mater. 20 (1984) 410.
[5] A.C.T. North, D.C. Phillips, F.S. Mathews, Acta Crystallogr. A 24 (1968) 351.
[6] G.M. Sheldrick, SHELXS-86 Program for the Solution of Crystal Structures, University of Göttingen, Germany, 1990.
[7] G.M. Sheldrick, SHELXL-97 Program for Crystal Structure Determination, University of Göttingen, Germany, 1997.
[8] M. Gabelica-Robert, M. Goreaud, Ph. Labbé, B. Raveau, J. Solid State Chem. 45 (1982) 389.
[9] Hok Nam Ng, C. Calvo, Can. J. Chem. 51 (1973) 2613.
[10] H. Boughzala, T. Jouini, J. Solid State Chem. 142 (1999) 104–110.
[11] I.D. Brown, D. Altermatt, Acta Crystallogr. B 41 (1985) 244.
[12] W.H. Baur, Acta Crystallogr. B 30 (1974) 1195–1215.
[13] D. Corbridge, Bull. Soc. Fr. Miner. Crist. 94 (1971) 271.
[14] L.K. Elbouaanani, B. Malaman, R. Gerardin, M. Ijjaali, J. Solid State Chem. 163 (2002) 412–420.
[15] K.H. Lii, N.S. Wen, C.C. Su, B.R. Chueh, Inorg. Chem. 31 (1992) 439–442.
[16] A. Grandin, A. Leclaire, M.M. Borel, B. Raveau, J. Solid State Chem. 115 (1995) 521–524.
[17] E. Dvoncova, K.-H. Lii, C.-H. Lii, T.-M. Chen, J. Solid State Chem. 106 (1993) 485.
[18] M. Rochere, A. Kahn, F. D'Yvoire, E. Bretey, Mater. Res. Bull. 20 (1985) 27–34.
[19] H. Boughzala, T. Jouini, Acta Crystallogr. C 54 (1998) 1731–1733.
[20] J.M. Winand, C. R. Acad. Sci. Paris, Sér. II 309 (1990) 1475–1480.
[21] S. Ledain, A. Leclaire, M.M. Borel, M. Hervieu, J. Provost, B. Raveau, J. Solid State Chem. 144 (1999) 297–310.
[22] J.M. Winand, A. Rulmont, P. Tarte, J. Solid State Chem. 87 (1990) 83–87.
[23] Y.F.Y. Yao, J.T. Kummer, J. Inorg. Nucl. Chem. 29 (1967) 2453.
[24] J.B. Goodenough, H.-Y.P. Hong, J.A. Kafalas, Mater. Res. Bull. 11 (1976) 203.